

Article

Development of an Enhanced Selective Harmonic Elimination for a Single-Phase Multilevel Inverter with Staircase Modulation

Govind S. ¹, Anilkumar Chappa ^{2,*}, K. Dhananjay Rao ³, Subhojit Dawn ³ and Taha Selim Ustun ^{4,*}¹ Department of Electrical Engineering, National Institute of Technology Raipur, Raipur 492010, India² Department of Electrical & Electronics Engineering, Sri Vasavi Engineering College (Autonomous), Tadepalligudem 534101, India³ Department of Electrical & Electronics Engineering, Velagapudi Ramakrishna Siddhartha Engineering College, Vijayawada 520007, India⁴ Fukushima Renewable Energy Institute, AIST (FREA), Koriyama 963-0298, Japan

* Correspondence: anilkumar.chappa201@gmail.com (A.C.); selim.ustun@aist.go.jp (T.S.U.)

Abstract: A low device switching frequency is recommended for the operation of multilevel inverters (MLIs) to achieve reduced switching losses. Selective harmonic elimination (SHE) and total harmonic distortion (THD) minimization are the two primary switching angle estimation methodologies for low-frequency modulation control. In this regard, a new generalized condition has been developed in this paper for the SHE technique. This original condition will give an output voltage with improved THD in comparison to the conventional SHE technique, while achieving its primary objective of eliminating the specific harmonic content from the output voltage. The proposed condition has been formulated by estimating the error associated with the staircase waveform and the desired sinusoidal output at the fundamental frequency. An infinite harmonic count has been considered for the evaluation of the quality of output, to obtain an accurate THD value without any underestimation. The proposed technique is analyzed, and its critical features are studied in Simulink. The effectiveness of the present work has been also validated by the experimental results.

Keywords: multilevel inverter (MLI); selective harmonic elimination (SHE); total harmonic distortion (THD); staircase modulation; cumulative absolute error (CAE)



Citation: S., G.; Chappa, A.; Rao, K.D.; Dawn, S.; Ustun, T.S.

Development of an Enhanced Selective Harmonic Elimination for a Single-Phase Multilevel Inverter with Staircase Modulation. *Electronics* **2022**, *11*, 3902. <https://doi.org/10.3390/electronics11233902>

Academic Editors: Ahmed Abu-Siada and Jingyang Fang

Received: 15 September 2022

Accepted: 22 November 2022

Published: 25 November 2022

Publisher's Note: MDPI stays neutral with regard to jurisdictional claims in published maps and institutional affiliations.



Copyright: © 2022 by the authors. Licensee MDPI, Basel, Switzerland. This article is an open access article distributed under the terms and conditions of the Creative Commons Attribution (CC BY) license (<https://creativecommons.org/licenses/by/4.0/>).

1. Introduction

In recent years, there has been an exponential rise in industrial sectors that demand high-power devices [1]. Connecting a conventional two-level inverter for a medium voltage grid is difficult, due to the increased voltage stress on power semiconductor switches. To overcome this difficulty, the concept of multilevel converters was introduced as a feasible and viable alternative [2]. To achieve higher power, the MLIs try to produce a staircase voltage waveform by utilizing power semiconductor switches in series with lower voltage dc sources. Batteries, renewable energy sources and capacitors can be used as multiple dc voltage sources [3–5]. MLIs are of great significance in medium- and high-voltage applications [3,6–8], where the quality of output is critical. MLIs have the capability to operate at the fundamental switching frequency and higher switching frequencies. To attain improved performance of MLIs, the low device switching frequency is employed [9]. The key step in employing the low-frequency modulation control is to choose the switching angles.

Selective Harmonic Elimination (SHE) and Total Harmonic Distortion (THD) minimization are the two major switching angle estimation approaches [8]. SHE is a feasible and practical alternative compared to the other modulation techniques which are used in variable speed drives or ground power units, due to the numerous advantages offered by the technique such as direct control over output waveform harmonics [10]. When SHE is

applied in a Cascaded H-Bridge (CHB), it becomes capable of performing in modular high-power electronics applications, such as electric vehicle charging stations [11]. A CHB with SHE has the capability to inject particular high-order harmonics in order to compensate for grid high-order harmonics. It is due to the above-mentioned reasons that the SHE technique has been extensively studied by the research community. A significant amount of work has been done in the SHE technique [12–17], which can completely eradicate low-order harmonics. Unfortunately, the approach is flawed from the perspective of THD reduction. In [18], a hybrid improved Particle Swarm Optimization (PSO)-Tabu Search (TS) algorithm is proposed to solve the non-linear equations to find the switching angles. In [19], the crystal structure algorithm (CryStA) is applied for implementing the SHE modulation technique in CHB MLI. The grasshopper optimization algorithm (GOA) has been used to implement SHE in [20]. In [21], a hybrid APSO algorithm has been implemented to estimate switching angles for SHE. Lastly, a bio-inspired intelligent algorithm (BIA) for implementing SHE in CHB MLI has been developed in [22]. However, the proposed technique, rather than solving for the non-linear SHE equations, proposes a new objective function that uses the SHE equations as constraints. The SHE technique implemented results in achieving SHE at reduced THDs.

In this paper, the objective is to improve upon the SHE technique by enhancing its output with regards to THD. In this paper, a new condition has been introduced for estimating switching angles for the SHE technique. This new condition will provide output with improved THD, while achieving its objective of eliminating the specific harmonic content from the output. This technique can be employed for any single-phase MLI topology operating at low switching frequency, with the aim of achieving minimal output voltage THD, along with achieving the required SHE. An inductively dominated RL-load is used for analysis, and the infinite harmonic count is considered during the evaluation of the quality of output to obtain an accurate THD value without any underestimation [23].

The rest of the paper has been organized as follows. Section 2 discusses the conventional SHE technique problem formulation, the development of the proposed strategy and the proposed problem formulation. Section 3 contains the analysis of the theoretical development. Section 4 consists of the simulation results. Section 5 discusses the experimental workbench, and the experimental results are tabulated. Section 6 discusses the conclusion of the present paper.

2. Methodology

In this section, the approach towards the proposed strategies' problem formulation is discussed. The problem formulation for conventional SHE has been presented. The development of the original condition has been explained, leading to the problem formulation of the proposed technique.

2.1. Conventional SHE

The conventional SHE, also referred to as the fundamental switching frequency method, is based on the harmonic elimination theory [24,25]. With an appropriate choice of conducting angles, the harmonic content can be removed without the use of an additional filter. One degree of freedom is used, so that the magnitude of the fundamental waveform corresponds to the reference waveform's amplitude or modulation index (m), as shown in (1). The modulation index (m) is the ratio of the amplitude of the fundamental component of output voltage to the step size of the multilevel output.

For a seven-level single-phase inverter (see Figure 1), the conducting angles β_1 , β_2 and β_3 (Figure 2) can be chosen to cancel the predominant lower-frequency harmonics.

$$\frac{4}{\pi} \{ \cos(\beta_1) + \cos(\beta_2) + \cos(\beta_3) \} = m \quad (1)$$

$$\cos(3\beta_1) + \cos(3\beta_2) + \cos(3\beta_3) = 0 \quad (2)$$

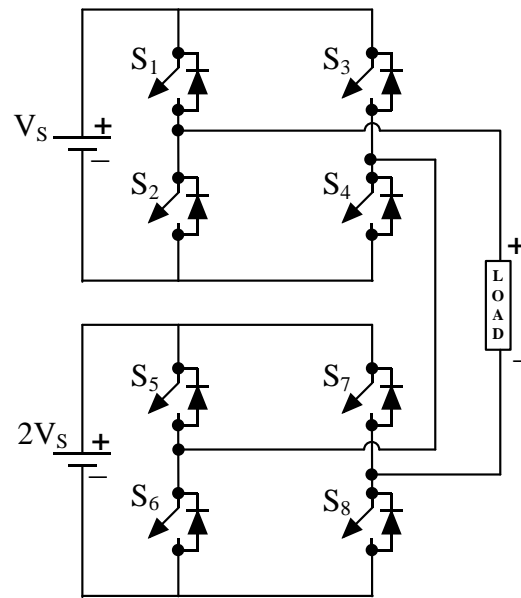


Figure 1. Quasi-linear MLI (n = 7).

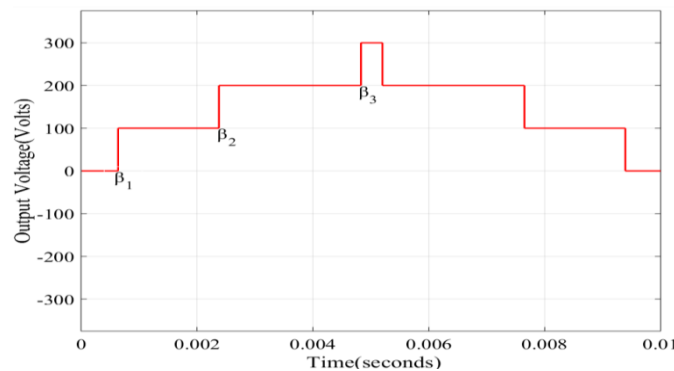


Figure 2. Output voltage half wave for the Quasi-linear seven level MLI.

Equation (2) is used to eliminate the third-order harmonic content from the output. These transcendental equations can be effectively deciphered using the MATLAB.

2.2. Development of the THD Reduction Constraint

The THD value for any signal is an index used to represent the extent of the absence of fundamental components present in the signal. Thus, for achieving a reduced THD, the staircase output of the MLI should approach a sinusoidal signal, with an amplitude and frequency the same as the fundamental component. An n-level MLI will have $((n - 1))/2$ conducting angles, and estimating switching angles properly is of huge significance. These switching angles can be estimated so as to achieve different objectives, including selective harmonic elimination and THD reduction. For achieving the THD reduction constraint, the deviation of the staircase waveform from the required desirable fundamental sinusoidal component has to be calculated. This deviation is minimized, and should result in an output with a reduced THD value. For the error calculation, the absolute error between the staircase waveform and the required fundamental component (see Figure 3) at all data points within the quarter wave time interval (due to the quarter wave symmetry exhibited by the waveforms) was calculated. The absolute error was then cumulatively added to obtain the cumulative absolute error over the quarter wave interval. This error estimation allows for equal importance to error value at all data points, irrespective of the magnitude of the error. For the purpose of obtaining the cumulative error, the area under each of the signals in question was calculated over the quarter wave interval, and

its difference was evaluated. Figure 4 depicts the code for implementing the proposed switching technique.

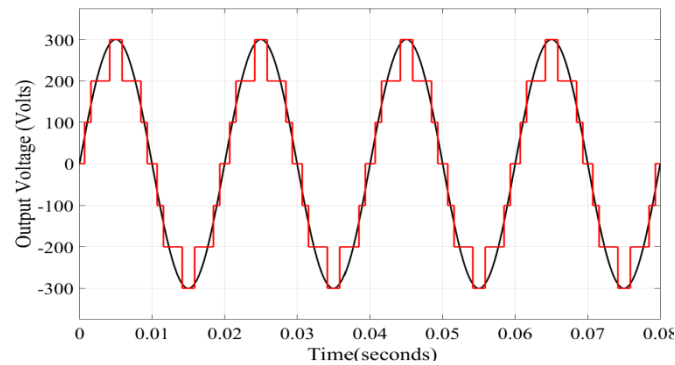


Figure 3. Seven-level MLI output voltage and fundamental component of output voltage both have quarter wave symmetry.

```

for ind=1:9
LB=[0;asin(1/t(ind));asin(2/t(ind))];
UB=[(asin(1/t(ind)));asin(2/t(ind));(pi/2)];
[X,fit]= fmincon(@ (X) obj_function(X,ind),X0,A,B,Aeq,Beq,LB,UB,@ (X) nonlcon(X,ind) \
options);
fit=(sqrt(2*fit)/t(ind))*100;
X=X*180/pi;
thd(i)=fit;
f1(i)=X(1);
f2(i)=X(2);
f3(i)=X(3);
i=i+1;
end
plot(t,thd,'k');

```

Figure 4. Code implementation of the proposed technique. The objective function and the constraints passed through the fmincon function.

Let A_1 be the area under the staircase waveform over the quarter wave time interval given by (3) and v be the staircase waveform. Then,

$$A_1 = \int_0^{\frac{\pi}{2}} v \, d\beta \tag{3}$$

$$A_1 = \int_{\beta_p}^{\frac{\pi}{2}} v \, d\beta + \int_{\beta_{p-1}}^{\beta_p} v \, d\beta + \dots + \int_0^{\beta_1} v \, d\beta$$

where p is the number of switching angles to be estimated for an n -level MLI given by (4)

$$p = \frac{n - 1}{2} \tag{4}$$

$$A_1 = \int_{\beta_p}^{\frac{\pi}{2}} pk \, d\beta + \int_{\beta_{p-1}}^{\beta_p} (p - 1)k \, d\beta + \dots$$

where k is the stepsize of the staircase output waveform, which is the dc voltage source value in a CHB.

$$A_1 = k[p\{(\pi/2) - \beta_p\} + (p - 1)\{\beta_p - \beta_{p-1}\} + \dots + \{\beta_2 - \beta_1\}] \tag{5}$$

Let A_2 be the area under the fundamental component over the quarter wave time interval given by (6). Then,

$$A_2 = \int_0^{\frac{\pi}{2}} (F_a \sin \beta) d\beta = F_a \quad (6)$$

where F_a is the amplitude of the fundamental component waveform, and now the cumulative absolute error (CAE) for an n -level MLI, E_n is given by (7):

$$E_n = A_2 - A_1 \quad (7)$$

Substituting (6) and (5) in (7):

$$E_n = F_a + k\{(\beta_1 + \beta_2 + \dots + \beta_p) - \left(\frac{\pi}{2}p\right)\} \quad (8)$$

$$E_n = k\{m + (\beta_1 + \beta_2 + \dots + \beta_p) - \left(\frac{\pi}{2}p\right)\} \quad (9)$$

Equations (10), (11) and (12) are the CAE equations for 5, 7 and 9-level MLI, respectively:

$$E_5 = k\{m + (\beta_1 + \beta_2) - \left(\frac{2\pi}{2}\right)\} \quad (10)$$

$$E_7 = k\{m + (\beta_1 + \beta_2 + \beta_3) - \left(\frac{3\pi}{2}\right)\} \quad (11)$$

$$E_9 = k\{m + (\beta_1 + \beta_2 + \beta_3 + \beta_4) - \left(\frac{4\pi}{2}\right)\} \quad (12)$$

2.3. Problem Formulation

For an n -level MLI, Equation (9) has to be plugged in while solving the switching angles using the SHE equations. The modulation index (m) term in the CAE equation ensures control over the amplitude of the fundamental component. The k value used for analysis and simulation is 100. An m value of 2.5 represents the amplitude of the fundamental component as 250. The MATLAB/*fsolve* function is used for effectively solving transcendental equations. The THD associated with both the classical SHE method and the proposed SHE method with the CAE equation has to be evaluated for comparison. The THD is calculated as per the equation evaluated in [26] for a several-level MLI with three switching angles.

3. Analysis of Theoretical Development

In this section, the theoretical development discussed in the previous sections will be analyzed. Different cases have been considered for this analysis. A general variation in THD has been plotted over the restricted modulation index, where the solution for SHE equations exists; this has been done for comparison purposes. In each case, two operating points have been selected to further discuss the effect of the newly developed constraint on switching angle estimation. The different cases considered are discussed below:

3.1. Third Order Harmonic Elimination

The proposed technique outperforms the restricted modulation index with regards to the distortion associated with the output voltage, as depicted in Figure 5. From Figure 6, it becomes evident that the proposed technique meets the requirement of eliminating the 3rd-order harmonics, along with reducing the THD associated with the output voltage at the same modulation index value ($m = 2.52$). Comparing Figure 6a,b, it can be observed that there is a variation in the harmonic content other than the eliminated 3rd harmonic. An increase in the 7th-order harmonic can be observed along with the reduction in both 5th

and 9th order harmonics in the results obtained from the proposed technique at $m = 2.52$. These variations are not controlled, and occur because of the THD reduction constraint. The variations in harmonic content other than the harmonic order selected for elimination have no particular trend, and thus it can be concluded that the THD reduction has been achieved by random suppression of harmonic contents present in the output voltage. Figure 7 shows the variation in the estimated switching angle for the two techniques, mentioned above. From Figure 6, it can be observed that the higher of the three switching angles, β_3 , does overlap at various operating points, but the other switching angles are different over the restricted modulation index. Furthermore, in the switching angle β_2 , the angle values determined by the proposed technique are lesser compared to the conventional technique throughout the restricted modulation index range, and the polar opposite is observed in the case of switching angle β_1 . By applying the CAE equation to the problem formulation for the SHE for any particular harmonic content elimination, the estimation of the switching angles will now be performed by distributing the degrees of freedom among the SHE equations and the CAE equation. Thus, the results obtained will have an improved THD.

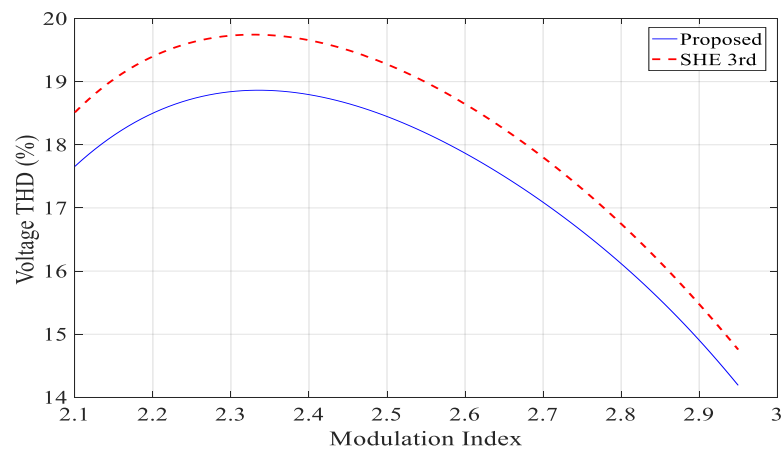


Figure 5. Curve showing variation between the Voltage THD in percent and modulation index for SHE of 3rd order harmonics and for the proposed technique.

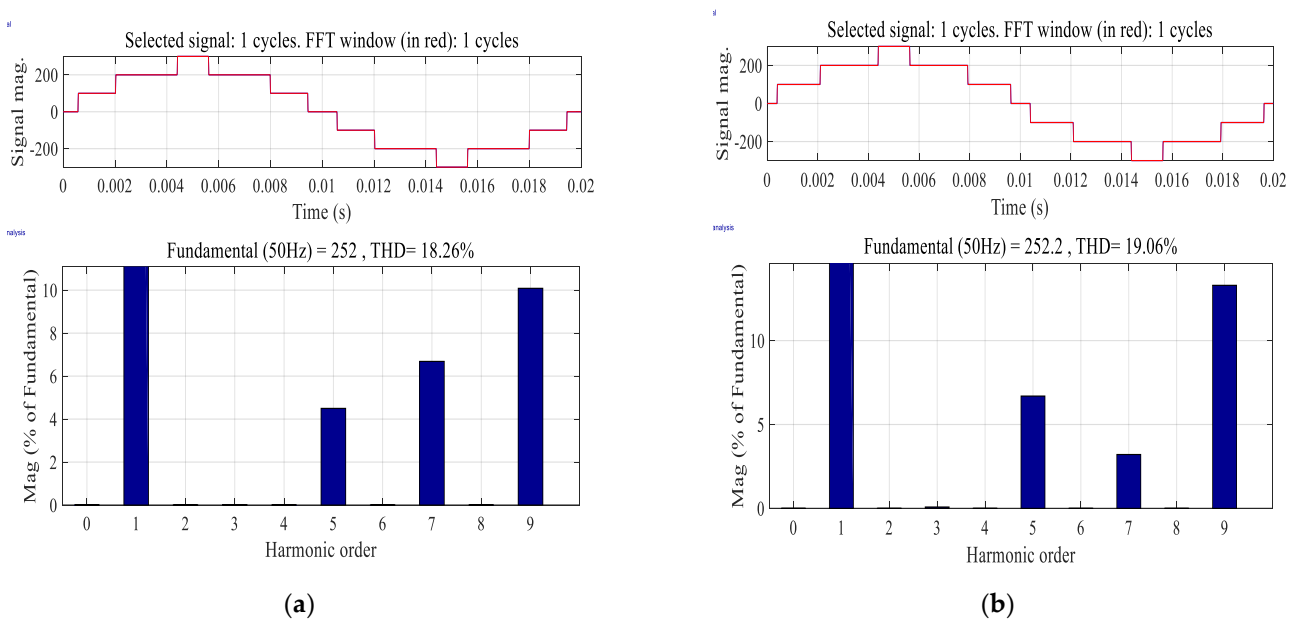


Figure 6. FFT analysis for 3rd order harmonic elimination at $m = 2.52$ using (a) the proposed technique and (b) the conventional technique.

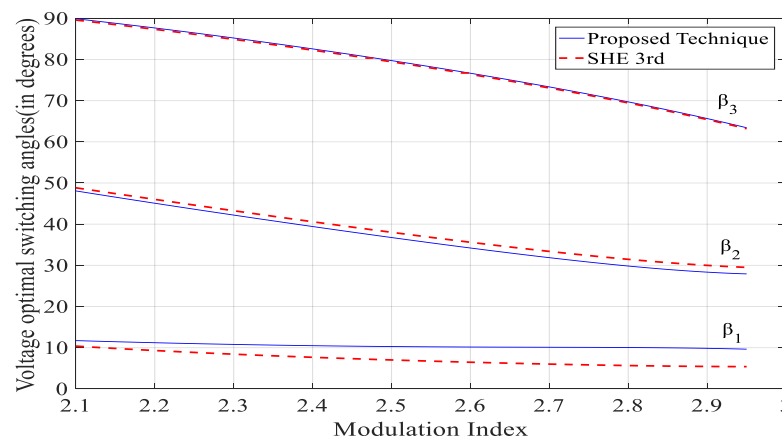


Figure 7. Curve showing variation between the estimated switching angles and modulation index for SHE of 3rd-order harmonics and the proposed technique.

3.2. Fifth Order Harmonic Elimination

The proposed technique has a reduced output voltage THD over the restricted modulation index, as depicted in Figure 8. From Figure 9, it is clear that the proposed technique is eliminating the 5th-order harmonics, along with reducing the THD of the output voltage at selected operating points ($m = 2.30$). From Figure 9, at $m = 2.30$ a natural cancellation of the 7th-order harmonic content can be observed, along with the cancellation of the target harmonic order in the case of the proposed technique. Additionally, it can be observed that the 3rd harmonic order has reduced significantly for the proposed technique, along with an increase in 9th-order harmonic content. This reduction in lower-order harmonic content other than the target harmonic has resulted in a significant reduction in THD of 3.90% for the proposed technique, in comparison to the conventional SHE technique. Figure 10 shows the variation in the estimated switching angle for the proposed and conventional 5th-order harmonic elimination techniques mentioned. From Figure 10, it can be seen that there is no overlap for any of the switching angles at any operating points. Except for switching the angle β_3 , the other switching angles are less for the proposed technique than compared to the conventional SHE.

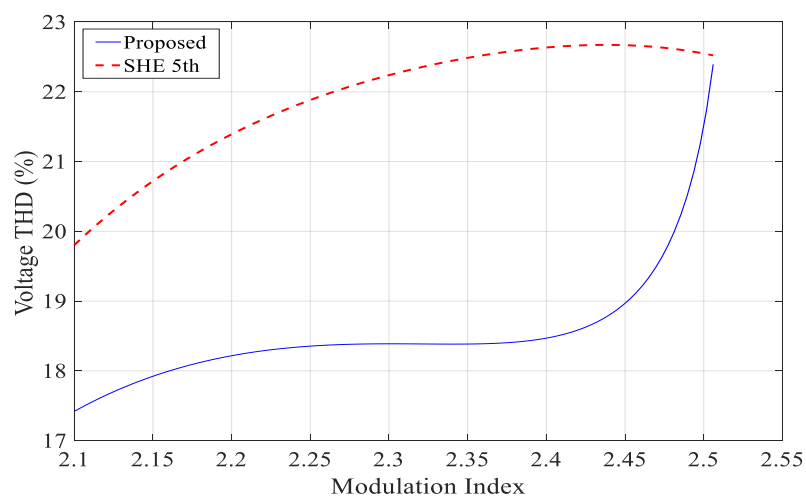


Figure 8. Curve showing variation between the Voltage THD in percent and modulation index for SHE of 5th order harmonics and for the proposed technique.

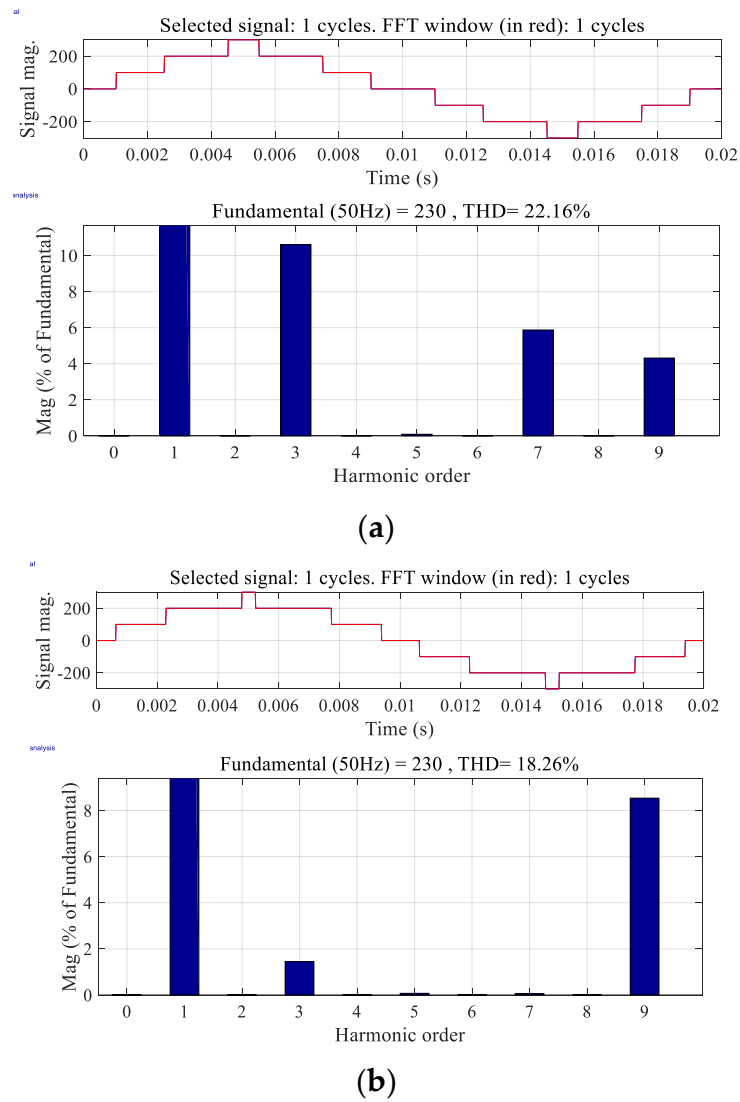


Figure 9. FFT analysis for 5th order harmonic elimination at $m = 2.30$ using (a) the conventional technique and (b) the proposed technique.

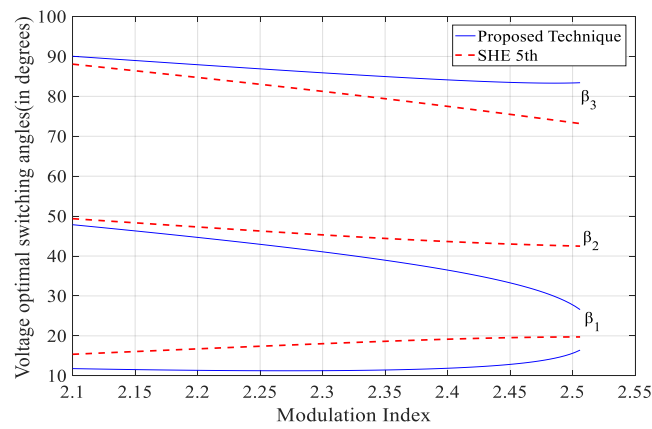


Figure 10. Curve showing variation between the estimated switching angles and modulation index for SHE of 5th-order harmonics and the proposed technique.

3.3. Ninth Order Harmonic Elimination

The proposed technique has a reduced output voltage THD over the restricted modulation index, as depicted in Figure 11. From Figure 12, it is clear that the proposed technique eliminates the 9th-order harmonics, along with reducing the THD of the output voltage at the two selected operating points ($m = 2.934$). From Figure 12, at $m = 2.934$, a reduction in THD of 3.94 can be observed; this can be attributed to the suppression of higher-order harmonics. Figure 13 shows the variation in the estimated switching angle for the two 9th-order harmonic elimination techniques mentioned. Moreover, the switching angle variations are more random, and all the switching angles do overlap at some operating points.

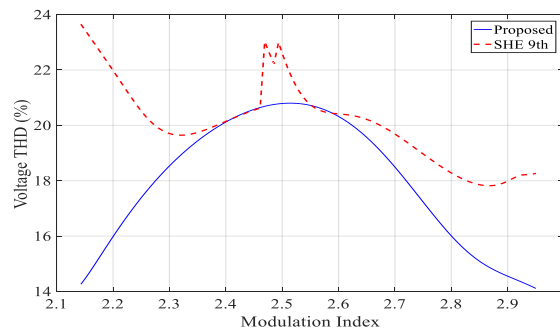


Figure 11. Curve showing variation between the Voltage THD in percent and modulation index for SHE of 9th order harmonics and for the proposed technique.

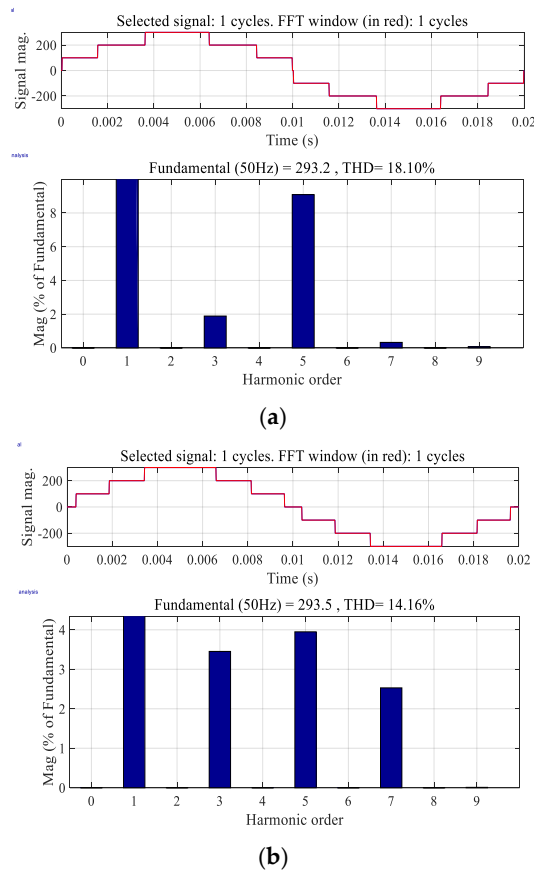


Figure 12. FFT analysis for 9th order harmonic elimination at $m = 2.934$ using (a) the conventional technique and (b) the proposed technique.

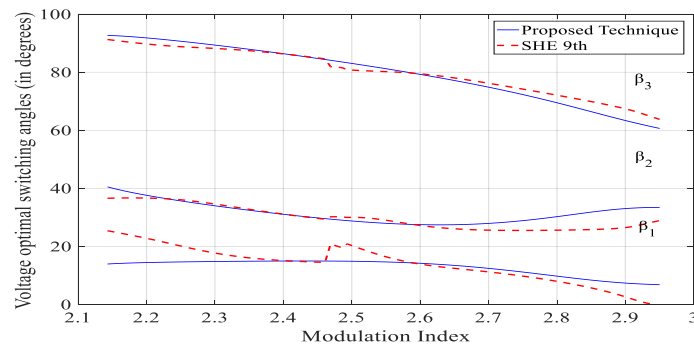


Figure 13. Curve showing variation between the estimated switching angles and modulation index for SHE of 9th-order harmonics and the proposed technique.

4. Simulation Results

Simulations were performed for verification of the analysis. Harmonic analysis of the output voltage was performed employing the MATLAB fast Fourier transform (FFT) tool for the various techniques presented. Four modulation indexes were selected for analysis. A quasi-linear MLI was implemented, considering the aforementioned points. Figure 14 shows the output of the Quasi-linear MLI implemented with an inductively dominated RL Load. The values of the voltage THDs of output voltage were obtained by performing the MATLAB simulations and carrying out the FFT analysis on the inverter output.

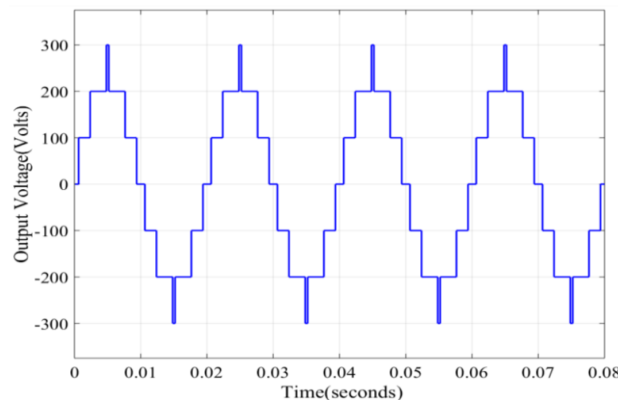


Figure 14. Output of the Quasi-linear MLI implemented with an inductively dominated RL Load.

The results have been tabulated (Tables 1–3) for the selected operating points for all the switching angle estimation methods considered.

Table 1. Simulation results for 3rd order harmonic elimination.

<i>m</i>	Conv. SHE		Prop. SHE	
	3rd-Order Harmonic Content Relative to Fundamental (%)	THD (%)	3rd-Order Harmonic Content Relative to Fundamental (%)	THD (%)
2.2631	0.02	19.55	0.01	18.68
2.435	0.05	19.46	0.06	18.61
2.607	0.11	18.53	0.09	17.72
2.9071	0.06	15.29	0.03	14.76
2.950	0.05	14.74	0.05	14.11

Conv-Conventional, Prop-Proposed

Table 2. Simulation results for 5th order harmonic elimination.

<i>m</i>	Conv. SHE		Prop. SHE	
	5th-Order Harmonic Content Relative to Fundamental (%)	THD (%)	5th-Order Harmonic Content Relative to Fundamental (%)	THD (%)
2.178	0.05	21.06	0.03	17.95
2.218	0.06	21.46	0.01	18.15
2.2599	0.05	21.81	0.03	18.26
2.35	0.03	22.43	0.03	18.31
2.425	0.01	22.54	0.05	18.54

Table 3. Simulation results for 9th order harmonic elimination.

<i>m</i>	Conv. SHE		Prop. SHE	
	9th-Order Harmonic Content Relative to Fundamental (%)	THD (%)	9th-Order Harmonic Content Relative to Fundamental (%)	THD (%)
2.297	0.08	19.67	0.06	18.42
2.623	0.06	21.46	0.01	18.15
2.754	0.01	18.87	0.05	17.02
2.8359	0.01	17.82	0.08	15.27
2.90	0.01	18.07	0.03	14.64

From the tabulated results, it is clear that the proposed technique has a reduced distortion in output compared to the conventional SHE. Additionally, it is also clear from the results that the specific harmonics were also removed in the proposed method.

5. Experimental Verification

A single-phase seven-level inverter has been implemented using the hybrid quasi-linear multilevel topology for performing experimental verification. The proposed technique was applied for SHE of 3rd and 9th. The obtained results were compared with the conventional SHE of 3rd and 9th, respectively, on the same modulation index value. For 3rd order, a harmonic elimination experiment was performed at $m = 2.52$ for both conventional and proposed techniques. Similarly, $m = 2.934$ were selected as operating points to do experimental verification for 9th order harmonic elimination, respectively. The obtained results are tabulated and subject to verification with the theoretical and simulation results. The experimental system is depicted in Figure 15. It consists of a TMDSDOCK28335 real-time digital controller, which is used to generate the desired gating pulses, a FLUKE 434-II power quality analyzer, which is used to analyze the THD spectrum, a HMP4030 programmable power supply that is used for DC power supply and a scope coder YOKOGAWA DL850E to record different output waveforms. The consider parameters for experimentation are $V_{DC1} = 100$ V, $V_{DC2} = 200$ V, and Impedance (Z) = $20 + j20$ Ω .

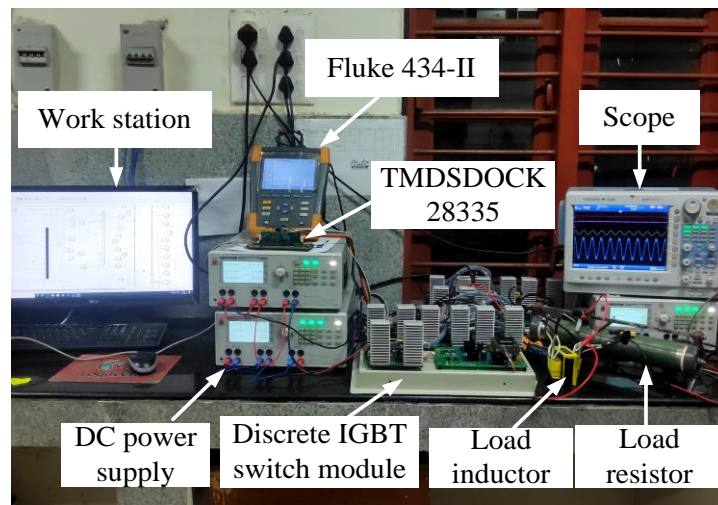
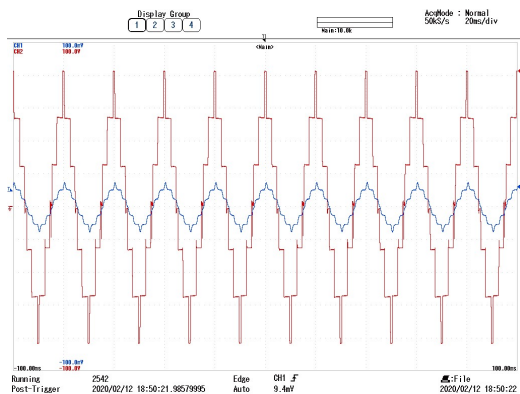
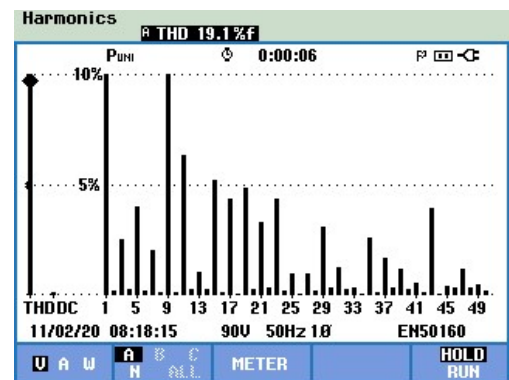


Figure 15. Experimental system.

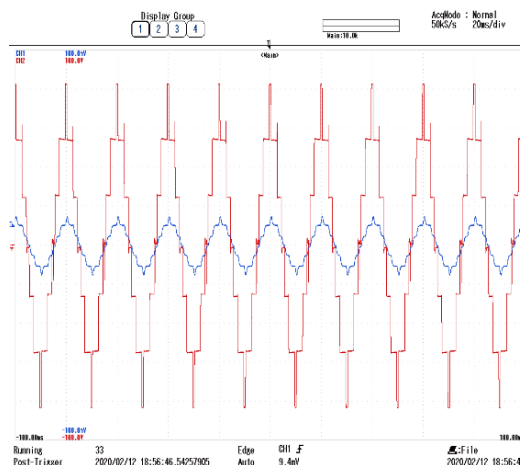
The output voltage waveforms for 3rd and 9th order harmonic elimination obtained from experimental hardware setup using both conventional and proposed techniques are shown in Figures 16 and 17.



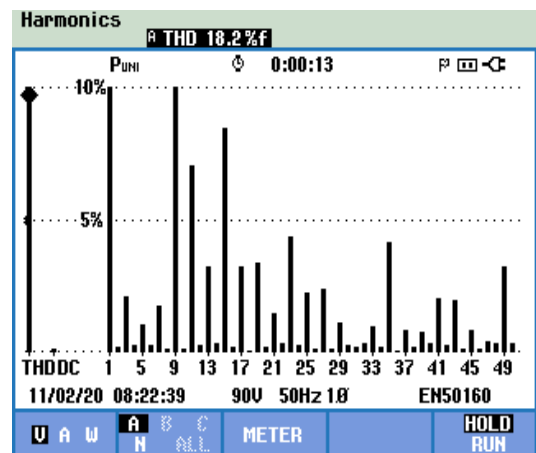
(a)



(b)

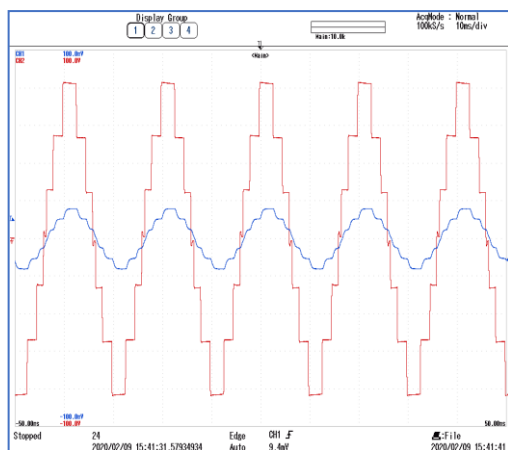


(c)

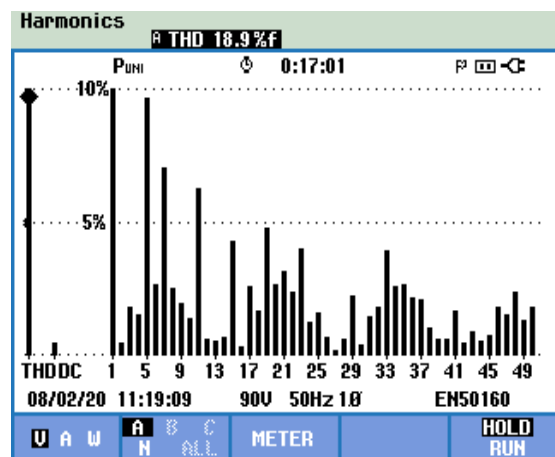


(d)

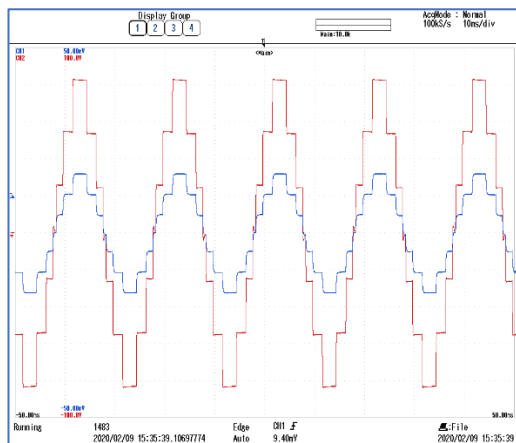
Figure 16. Hardware result of the Quasi-linear MLI for 3rd order harmonic elimination using: (a) the conventional technique; (b) THD analysis of the conventional technique; (c) the proposed technique; and (d) THD analysis of the proposed technique.



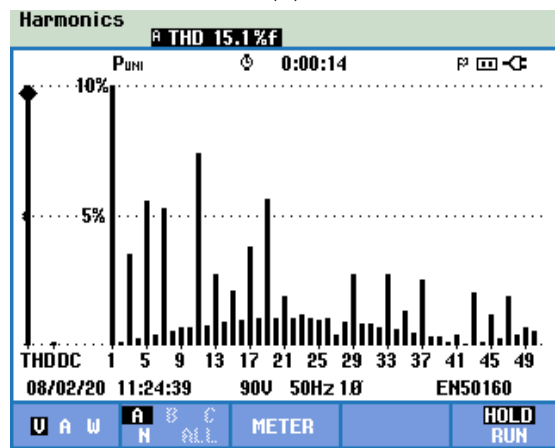
(a)



(b)



(c)



(d)

Figure 17. Hardware result of the Quasi-linear MLI for 9th order harmonic elimination using: (a) the conventional technique; (b) THD analysis of the conventional technique; (c) the proposed technique; and (d) THD analysis of the proposed technique.

6. Conclusions

A novel SHE-switching angle determination technique with a new condition is proposed in this paper. The problem has been formulated as a non-linear system of equations. The variation in voltage THD between the proposed technique and the conventional technique was analyzed over the specific modulation index range by theoretical analysis. The proposed approach was found to reduce the distortion in the output voltage in comparison to conventional SHE. The switching angles estimated by the proposed strategy provide an improved THD output voltage over conventional SHE. Simulations performed at different modulation indices proved the effectiveness of the proposed method in attaining the primary goal of SHE and the additional aim of THD reduction. The experimental workbench has been designed to validate the theoretical and simulation results.

Author Contributions: Conceptualization, G.S.; Methodology, A.C.; Formal analysis, K.D.R.; Investigation, T.S.U.; Data curation, S.D.; Project administration, T.S.U.; Funding acquisition, T.S.U. All authors have read and agreed to the published version of the manuscript.

Funding: This research received no external funding.

Conflicts of Interest: The authors declare no conflict of interest.

References

1. Ustun, T.S.; Hashimoto, J.; Otani, K. Impact of Smart Inverters on Feeder Hosting Capacity of Distribution Networks. *IEEE Access* **2019**, *7*, 163526–163536. [[CrossRef](#)]
2. Baker, R.H.; Bannister, L.H. Electric Power Converter. US3867643A, 18 February 1975. pp. 1–17.
3. Rodríguez, J.; Member, S.; Lai, J.; Member, S. Multilevel Inverters: A Survey of Topologies, Controls, and Applications. *IEEE Trans. Ind. Electron.* **2002**, *49*, 724–738. [[CrossRef](#)]
4. Lai, J.; Peng, F.Z. Multilevel converters—a new breed of power converters. *IEEE Trans. Ind. Appl.* **1996**, *32*, 509–517.
5. Tolbert, L.M.; Peng, F.Z.; Habetler, T.G. Multilevel converters for large electric drives. *IEEE Trans. Ind. Appl.* **1999**, *35*, 36–44. [[CrossRef](#)]
6. Buccella, C.; Cecati, C.; Cimatorini, M.G.; Razi, K. Analytical method for pattern generation in five-level cascaded H-bridge inverter using selective harmonic elimination. *IEEE Trans. Ind. Electron.* **2014**, *61*, 5811–5819. [[CrossRef](#)]
7. Mora, A.; Lezana, P.; Juliet, J. Control scheme for an induction motor fed by a cascade multicell converter under internal fault. *IEEE Trans. Ind. Electron.* **2014**, *61*, 5948–5955. [[CrossRef](#)]
8. Edpuganti, A.; Rathore, A.K. Fundamental Switching Frequency Optimal Pulsewidth Modulation of Medium-Voltage Cascaded Seven-Level Inverter. *IEEE Trans. Ind. Appl.* **2015**, *51*, 3485–3492. [[CrossRef](#)]
9. Tarisciotti, L.; Zanchetta, P.; Watson, A.; Bifaretti, S.; Clare, J.C. Modulated model predictive control for a seven-level cascaded h-bridge back-to-back converter. *IEEE Trans. Ind. Electron.* **2014**, *61*, 5375–5383. [[CrossRef](#)]
10. Tang, T.; Han, J.; Tan, X. Selective harmonic elimination for a cascade multilevel inverter. In Proceedings of the 2006 IEEE International Symposium on Industrial Electronics, Montreal, QC, Canada, 9–13 July 2006; Volume 2, pp. 977–981.
11. Haghdar, K. Optimal DC Source Influence on Selective Harmonic Elimination in Multilevel Inverters Using Teaching-Learning Based Optimization. *IEEE Trans. Ind. Electron.* **2019**, *46*, 1. [[CrossRef](#)]
12. Inverters, S.F. Self-Elimination of Triplen Harmonics for. *IEEE Trans. Power Electron.* **2019**, *34*, 86–96.
13. Chiasson, J.N.; Tolbert, L.M.; McKenzie, K.J.; Du, Z. Elimination of Harmonics in a Multilevel Converter Using the Theory of Symmetric Polynomials and Resultants. *IEEE Trans. Control Syst. Technol.* **2005**, *13*, 216–223. [[CrossRef](#)]
14. Du, Z.; Member, S.; Tolbert, L.M.; Member, S.; Chiasson, J.N.; Member, S. Active Harmonic Elimination for Multilevel Converters. *IET Power Electron.* **2006**, *21*, 459–469.
15. Dahidah, M.S.A.; Konstantinou, G.; Agelidis, V.G. A Review of Multilevel Selective Harmonic Elimination PWM: Formulations, Solving Algorithms, Implementation and Applications. *IEEE Trans. Power Electron.* **2015**, *30*, 4091–4106. [[CrossRef](#)]
16. Wells, J.; Nee, B.; Chapman, P.; Krein, P. Selective Harmonic Control: A General Problem Formulation and Selected Solutions. *IEEE Trans. Power Electron.* **2005**, *20*, 1337–1345. [[CrossRef](#)]
17. Sharifzadeh, M.; Member, S.; Vahedi, H.; Member, S. New Constraint in SHE-PWM for Single-Phase Inverter Applications. *IEEE Trans. Ind. Appl.* **2018**, *54*, 4554–4562. [[CrossRef](#)]
18. Li, Y.; Zhang, X.-P.; Li, N. An Improved Hybrid PSO-TS Algorithm for Solving Nonlinear Equations of SHEPWM in Multilevel Inverters. *IEEE Access* **2022**, *10*, 48112–48125. [[CrossRef](#)]
19. Farooqui, S.A.; Shees, M.M.; Alsharekh, M.F.; Alyahya, S.; Khan, R.A.; Sarwar, A.; Khan, S. Crystal Structure Algorithm (CryStAl) Based Selective Harmonic Elimination Modulation in a Cascaded H-Bridge Multilevel Inverter. *Electronics* **2020**, *10*, 3070. [[CrossRef](#)]
20. Steczek, M.; Jefimowski, W.; Szeląg, A. Application of grasshopper optimization algorithm for selective harmonics elimination in low-frequency voltage source inverter. *Energies* **2020**, *13*, 6426. [[CrossRef](#)]
21. Memon, M.A.; Mekhilef, S.; Mubin, M. Selective harmonic elimination in multilevel inverter using hybrid APSO algorithm. *IET Power Electron.* **2018**, *11*, 1673–1680. [[CrossRef](#)]
22. Rai, N.; Chakravorty, S. Generalized formulations and solving techniques for selective harmonic elimination PWM strategy: A review. *J. Inst. Eng.* **2019**, *100*, 649–664. [[CrossRef](#)]
23. Short, T.A. *Electric Power Distribution Handbook*; CRC Press: Boca Raton, FL, USA, 2014.
24. Hoft, R.G. Generalized Techniques of Harmonic Elimination and Voltage Control in Thyristor Inverters: Part I—Harmonic Elimination. *IEEE Trans. Ind. Appl.* **1973**, *3*, 210–317.
25. Patel, H.S.; Hoft, R.G. Generalized techniques of harmonic elimination and voltage control in thyristor inverters part II—Voltage control techniques. *IEEE Trans. Ind. Appl.* **1974**, *IA-10*, 666–673. [[CrossRef](#)]
26. Srndovic, M.; Familiant, Y.L.; Grandi, G.; Ruderman, A. Time-Domain Minimization of Voltage and Current Total Harmonic Distortion for a Single-Phase Multilevel Inverter with a Staircase Modulation. *Energies* **2016**, *9*, 815. [[CrossRef](#)]